ehp ENVIRONMENTAL HEALTH PERSPECTIVES

ehponline.org

Low-level Mercury Can Enhance Procoagulant Activity of Erythrocytes: A New Contributing Factor for Mercury-related Thrombotic Disease

Kyung-Min Lim, Sujin Kim, Ji-Yoon Noh, Keunyoung Kim, Won-Hee Jang, Ok-Nam Bae, Seung-Min Chung, Jin-Ho Chung

doi: 10.1289/ehp.0901473 (available at http://dx.doi.org/)
Online 23 March 2010

NIEHS
National Institute of Environmental Health Sciences

National Institutes of Health
U.S. Department of Health and Human Services

Low-level Mercury Can Enhance Procoagulant Activity of Erythrocytes: A New Contributing Factor for Mercury-related Thrombotic Disease

Kyung-Min Lim[1,2], Sujin Kim[1,2], Ji-Yoon Noh, Keunyoung Kim, Won-Hee Jang, Ok-Nam Bae, Seung-Min Chung, and Jin-Ho Chung

College of Pharmacy, Seoul National University, Seoul 151-742, Korea

[1] These authors contributed equally.

[2] Current address: R&D Center, Amorepacific Co, Gyeonggi-do 446-729, Korea

Address correspondence to Jin-Ho Chung, College of Pharmacy, Seoul National University, Shinrim-dong San 56-1, Seoul 151-742, Korea
Tel: +82-2-880-7856
Fax: +82-2-885-4157
E-mail: jhc302@snu.ac.kr

Running title: Procoagulant Activation of Erythrocytes by Mercury

Key words: erythrocyte, mercury, phosphatidylserine exposure, procoagulant activity

Acknowledgements: This research was supported by a grant from Korea Food & Drug Administration in 2010.

Competing Financial Interests Declaration: None

Abbreviations: ACD, acid citrate dextrose; BSA, bovine serum albumin; C_6-NBD-PC, 1-oleoyl-2-[6-[(7-nitro-2-1,3-benzoxadiazol-4-yl)amino]hexanoyl]-sn-glycero-3-phosphocholine; C_6-NBD-PS, 1-Palmitoyl-2-[6-[(7-nitro-2-1,3-benzoxadiazol-4-yl)amino]hexanoyl]-sn-glycero-3-phospho-L-serine; CVDs, cardiovascular diseases; DTT, dithiothreitol; MV, microvesicles; PBS, phosphate buffered saline; PS, phosphatidylserine; TBS, Tris buffered saline; TPEN, N,N,N‘,N-tetrakis(2-pyridylmethyl)ethylenediamine.

Abstract

Background: Associations between cardiovascular diseases (CVDs) and mercury have been frequently described, but underlying mechanisms are poorly understood.

Objectives: We investigated the procoagulant activation of erythrocytes, an important contributor to thrombosis, by low-level mercury to explore the roles of erythrocytes in mercury-related CVDs.

Methods: Freshly isolated human erythrocytes and *ex vivo* and *in vivo* thrombosis models in rats were used to investigate mercury-induced procoagulant activity.

Results: Prolonged exposure to low-dose Hg^{2+} (0.25 - 5 μM for 1 - 48 hrs) induced erythrocyte shape changes from discocytes to echinocytes to spherocytes accompanied by microvesicle (MV) generation. These MV and remnant erythrocytes expressed phosphatidylserine (PS), an important mediator of procoagulant activation. Hg^{2+} inhibited flippase, an enzyme that recovers PS into the inner leaflet of the cell membrane, and activated scramblase, an enzyme that alters lipid asymmetry in the cell membrane. Consistent with these activity changes, Hg^{2+} increased intracellular calcium and depleted ATP and protein thiol. Thiol supplement reversed Hg^{2+} -induced MV generation and PS exposure and inhibited Ca^{2+} increase and ATP depletion, indicating that free-thiol depletion was key to Hg^{2+} -mediated procoagulant activity. The procoagulant activity of Hg^{2+}-treated erythrocytes was demonstrated by increased thrombin generation and endothelial cell adhesion. Hg^{2+}-mediated procoagulant activation of erythrocytes was further confirmed in *ex vivo* and *in vivo* rat thrombosis models, where Hg^{2+} treatment (0.5 - 2.5 mg/kg) increased PS exposure and thrombus formation significantly.

Conclusion: This study demonstrated that mercury could provoke procoagulant activity

in erythrocytes through protein thiol depletion-mediated PS exposure and MV generation, ultimately leading to enhanced thrombosis.

Introduction

Mercury is a widely distributed heavy metal element in earth crust, sea water, fresh water and air (Environment Canada 2004). Concomitantly with modern industrialization, human exposure to mercury has increased through anthropogenic mercury emissions from fuel combustion, municipal incinerators and chemical industries. Mercury exposure is regarded to be a major environmental toxic metal throughout the world (Mahaffey and Mergler 1998; Salonen et al. 2000; Valera et al. 2008; ASTDR 2007) and a lot of efforts are being directed on reducing environmental mercury pollution (Trasande et al. 2005). Recent reports on the blood mercury level of New York City adults showed that mean blood mercury level is 2.73 μg/L, higher than blood lead or cadmium levels (McKelvey et al. 2007). Moreover, heavy fish consumers exhibited 3.7 times the blood mercury levels observed in those who reported no consumption and some people in the areas active in gold mining showed an extremely high level of blood mercury level, close to 150 μg/L (~0.75 μM) (Akagi et al. 1995), raising a strong concern over the mercury exposure problem.

Mercury is harmless in insoluble form but vapor or soluble forms such as inorganic mercury or methylmercury can be extremely toxic to humans. Most of human mercury exposure is achieved by inhalation of elemental mercury vapor released from dental amalgam and through the consumption of fish contaminated with methylmercury (Berlin et al. 2007). Once inhaled, elemental mercury vapor is rapidly accumulated into erythrocytes and undergoes oxidation to mercuric ion by catalase. Orally absorbed methylmercury is preferentially distributed into erythrocytes (~90%) and slowly turns into mercuric ion through demethylation in the spleen and liver. It has been demonstrated that 6 - 15% of total mercury in the blood of heavy fish consuming

populations exists in the form of inorganic mercury (Rodrigues et al. 2010; Berglund et al. 2005). Since elemental mercury or methylmercury ultimately turns into mercuric ion in body (Zalups 2000), mercuric salt has been commonly used to investigate the toxicity of mercury.

Mercury toxicity is mainly manifested as neuronal disorders, immunotoxicity and kidney damage (Clarkson et al. 2003), however, cardiovascular diseases (CVDs) including atherosclerosis, coronary heart diseases, pulmonary embolism, hypertension, and vessel obstruction have been also frequently described in relation to mercury exposure (Virtanen et al. 2007; Houston 2007; Virtanen et al. 2005). Previously, CVDs associated with mercury exposure have been assumed to occur as a consequence of renal effects of mercury, but increasing attention is also being given to direct effects of mercury on CV tissues including blood vessels, endothelial cells (Wiggers et al. 2008), platelets (Macfarlane 1981) and erythrocytes (Suwalsky et al. 2000). However, the role of direct toxic effects of mercury on CV tissues in the pathogenesis of mercury-associated CVDs has not been clarified yet.

Well characterized hemolytic and anemia-inducing effects of mercury suggest that the erythrocyte might be an important target of mercury (Zolla et al. 1997). Recently, Eisele et al. (2006) reported that low level Hg^{2+} exposure can induce phosphatidylserine (PS) translocation to the external surface of the erythrocyte cell membrane (i.e., PS exposure) through the modulation of clotrimazole-sensitive K^+ ion channel. They elaborated the PS-exposing effects of Hg^{2+} in relation to the apoptosis of erythrocytes. However, the implications of PS-externalized erythrocytes in procoagulant activation and subsequent CVDs were not addressed. Alterations of the erythrocyte membrane, including PS-exposure and PS-bearing microvesicle (MV) formation, can render

erythrocytes procoagulant, enabling the active participation of erythrocytes in thrombosis (Chung et al. 2007). PS exposed on erythrocytes provides a site for the assembly of the prothrombinase and tenase complex, leading to efficient thrombin generation and ultimately to clotting (Zwaal et al. 1977; Zwaal and Schroit 1997). Furthermore, increased adhesion of PS expressing erythrocytes to endothelial cells contributes to vaso-occlusion (Closse et al. 1999). MVs generated from deformed erythrocytes through vesiculation process also contribute to an acceleration of the coagulation cascade via strong procoagulant activity and by serving as a rich source of PS (Martinez et al. 2005).

In the current study, we discovered that both MV generation and PS exposure could be induced in human erythrocytes by low dose Hg^{2+} ($HgCl_2$, 0.25 – 5 μM). Of note, Hg^{2+}-mediated PS exposure and MV generation could enhance thrombin generation and adhesion to vascular endothelial cells, which is considered a direct marker for procoagulant activity. The mechanism underlying and *in vivo* relevancy of Hg^{2+}-induced procoagulant activation of erythrocytes was examined in an effort to give an insight into the CVDs associated with mercury exposure.

Materials and Methods

Materials

Mercury chloride($HgCl_2$), $CaCl_2$, ethylenediaminetetraacetic acid (EDTA), bovine serum albumin (BSA), KH_2PO_4, NaCl, Na_2HPO_4, KCl, Tris/HCl, $MgCl_2$, NaH_2PO_4, dextrose, sodium citrate, Tris-base, $NaHCO_3$, DMSO, ethanol, Triton X-100, trichloroacetic acid (TCA), Tris-acetate, ATP bioluminescent assay kit, iodoacetic acid, adenosine, EGTA, acetic acid, purified human thrombin, calcium ionophore A23187, and N,N,N‘,N-tetrakis(2-pyridylmethyl)ethylenediamine(TPEN) were obtained from Sigma chemical Co. (St. Louis, MO). Fluo-4-AM was from Molecular Probes (Eugene, OR) and Fluorescein-isothiocyanate (FITC)-labeled annexin V (annexin V-FITC) was from Pharmingen (San Diego, CA). Phycoerythrin-labeled monoclonal antibody against human glycophorin A (anti-glycophorin-A-RPE) was purchased from Dako Cytomation (Glostrub, Denmark). 1-Palmitoyl-2-[6-[(7-nitro-2-1, 3-benzoxadiazol-4-yl)amino] caproyl]-sn-glycero-3-phosphoserine (C_6-NBD-PS), and 1-oleoyl-2-[6-[(7-nitro-2-1,3-benzoxadiazol-4-yl)amino]hexanoyl]-sn-glycero-3-phosphocholine (C_6-NBD-PC) were purchased from Avanti Polar Lipids (Alabaster, AL). Purified human prothrombin, factor Xa and factor Va were bought from Hematologic Technologies, Inc. (Essex Junction, VT) and S2238 (chromogenic substrate for thrombin) was from Chromogenix (Milano, Italy). Human recombinant tissue factor (Recombiplastin) was from Instrumentation Laboratory (Lexington, MA) and other chemicals were of highest grade available.

Preparation of human erythrocytes

Human blood was obtained from healthy male donors (18-25 years old) using a vacutainer with acid citrate dextrose (ACD) and a 21-gauge needle (Becton Dickinson) on the day of each experiment. This study was approved by the Institutional Review Board at the Seoul National University/Health Service Center and all subjects provided written informed consent. Platelet rich plasma and buffy coat were removed by aspiration after centrifugation at 200 g for 15 min. Packed erythrocytes were washed 3 times with phosphate buffered saline (PBS: 1 mM KH_2PO_4, 154 mM NaCl, 3 mM Na_2HPO_4, pH 7.4) and once with Tris buffer (15 mM Tris-HCl, 150 mM NaCl, 5 mM KCl, 2 mM $MgCl_2$, pH 7.4) or Ringer solution (125 mM NaCl, 5 mM KCl, 1 mM $MgSO_4$, 32 mM HEPES, 5 mM glucose, pH 7.4). Washed erythrocytes were resuspended in Tris buffer or Ringer solution to a cell concentration of 5 x 10^7 cells/mL and final $CaCl_2$ concentration was adjusted to 1 mM prior to use.

Microscopic observation using scanning electron microscopy and confocal microscopy

After fixation with 2% glutaraldehyde solution for 1 hr at 4℃, the erythrocytes were centrifuged and washed 3 times with PBS, and followed by post-fixation with 1% osmium tetroxide for 30 min at room temperature. After washing with PBS several times, the samples were dehydrated serially with 50, 75, 90, and 100% ethanol. After drying and coating with gold, the images were observed on scanning electron microscope (JEOL, Japan). For confocal microscopy, 200 μL of erythrocytes suspension was added and attached for 1 hr to 8-chambered coverslip (Lab-Tek®) which has been coated with 0.1 mg/mL poly-L-lysine. After washing coverslip 3 times with TBS buffer

containing 2% BSA, erythrocytes were stained with TBS buffer containing anti-glycophorin-A-FITC for 30 min and washed 3 times again. Then, erythrocytes were incubated with vehicle (TBS) or Hg^{2+} and then observed using confocal microscopy equipped with argon laser (Leica, Wetzlar, Germany). Excitation and emission filters were set at 488 nm and 550-600 nm, respectively.

Flow cytometric analysis of phosphatidylserine exposure and cytosolic calcium in erythrocytes

Annexin V-FITC was used as a marker for phosphatidylserine (PS) positivity, while anti-glycophorin A-RPE was for an identifier of erythrocytes. Negative controls for annexin V binding were stained with annexin V-FITC in the presence of 2.5 mM EDTA instead of 2.5 mM $CaCl_2$. For detecting intracellular calcium increase, erythrocytes were loaded with 3 μM Fluo-4 AM for 1 hr at 37°C in the dark. Subsequently, the cells were washed twice and then resuspended in Tris buffer to a final concentration of 5 x 10^7 cells/mL with 1 mM of $CaCl_2$. For the confirmation of interference of Fluo-4 calcium signal by Hg^{2+}, TPEN (100 μM) was added for 5 min to extract Fluo-4 bound Hg^{2+}. To quench off extracellular calcium, 3 mM of EGTA was added to the erythrocyte suspension. Samples were analyzed on the flow cytometer FACScalibur™ (Becton Dickinson, San Diego, CA). Data from 10,000 events were collected and analyzed using CellQuest™ Pro software.

Phospholipid translocation measurement

Phospholipid translocation was measured according to the methods previously described by Hilarius et al. (2004). Briefly, erythrocytes (5×10^7 cells/mL) were

incubated with Hg^{2+} and then loaded with 0.5 μM C_6-NBD-PS (for the assay of flippase activity) or C_6-NBD-PC (for the assay of scramblase activity). Aliquots from the cell suspension were removed at the indicated time intervals and placed on cold Tris buffer and incubated on the ice for 10 min in the presence or absence of 1% bovine serum albumin (BSA) respectively. The amount of internalized probe was determined by comparing the fluorescence intensity associated with the cells before and after back-extraction. Samples were analyzed on the flow cytometer FACScalibur™ (Becton Dickinson).

Intracellular ATP level measurement

After incubation with Hg^{2+}, erythrocytes were washed and resuspended in Tris buffer containing 1 mM $CaCl_2$. The aliquot was mixed vigorously with 10% trichloroacetic acid solution and TAE buffer (100 mM Tris-acetate, 2 mM EDTA, pH 7.8) and then cooled in ice for 20 min. The sample was centrifuged and the aliquot of resultant supernatant was mixed with cold TAE buffer. Samples were adapted to luciferin/luciferase assay in Luminoskan (Labsystems, Franklin, MA) using an ATP assay kit (Sigma). The ATP concentrations were calculated based on the ATP standard curve.

Protein thiol level measurement

Protein thiol concentrations were determined by a modified assay based on the previously described colorimetric method (Di Monte et al. 1984). After incubation with various concentrations of Hg^{2+}, erythrocytes were centrifuged at 7,000 g for 1 min, and the supernatant was removed. The pellet was resuspended with lysis buffer (5 mM

sodium phosphate, pH 8) and incubated on ice for 30 min. Total lysate was resuspended with 5% perchloric acid on the ratio of 2 to 5, and then centrifuged at 7,000 g for 2 min. The pellet was solubilized in 1 mL of Tris-EDTA buffer (0.5 mM Tris-HCl, 5 mM EDTA, pH 7.6) containing 1% SDS. DTNB (250 μM) was added to the samples, and the change of the absorbance was measured at 412 nm. The content of protein thiol was calculated on the basis of a glutathione calibration curve and divided by the protein content, which was measured by Bio-Rad protein assay kit (Hercules, CA).

Prothrombinase assay

After incubation with Hg^{2+} for 4 hr, erythrocytes were incubated with 5 nM factor Xa and 10 nM factor Va in Tyrode buffer (134 mM NaCl, 10 mM HEPES, 5 mM glucose, 2.9 mM KCl, 1 mM $MgCl_2$, 12 mM $NaHCO_3$, 0.34 mM Na_2HPO_4, 0.3% BSA, 2 mM $CaCl_2$, pH 7.4) for 3 min at 37°C. Thrombin formation was initiated by addition of 2 μM prothrombin. Exactly 3 min after addition of prothrombin, an aliquot of the suspension was transferred to a tube containing stop buffer (50 mM Tris-HCl, 120 mM NaCl, 2 mM EDTA, pH 7.9). Thrombin activity was determined using the chromogenic substrate S2238. The rate of thrombin formation was calculated from the change in absorbance at 405 nm, using a calibration curve generated with active site-titrated thrombin.

Measurement of thrombin generation in plasma

Thrombin generation in plasma was measured according to the methods previously described by Peyrou et al. (1999). Briefly, Tris buffer or Hg^{2+} treated

erythrocytes were added to plasma and under gentle magnetic stirring, thrombin formation was initiated by adding Recombiplastin diluted (1:3,200) in Tris buffer containing 100 mM $CaCl_2$ to the mixture. After 10 min, the aliquots were collected and transferred to a Tris buffer containing 20 mM EDTA. The thrombin concentration was obtained as previously described in prothrombinase assay.

Adherence of erythrocytes to human umbilical vein endothelial cells

The human umbilical vein endothelial cells (HUVEC; 3 passages) were maintained in the EGM kit at 37^{o}C in a 95% air/5% CO_2 incubator. Before the experiments, 1 x 10^5 cells were seeded into T25 flask and grown for 5 days. Erythrocyte adherence to HUVEC was measured using modification of the methods described by Chung et al. (2007). PBS- or Hg^{2+}-treated erythrocytes were washed twice and resuspended in EBM-2 to a cell concentration of 5 x 10^7 cells/mL. After HUVEC was washed twice with EBM-2 to remove media, the erythrocytes were layered onto confluent HUVEC monolayer and incubated for 45 min at 37^{o}C. After the incubation, the flask was rinsed three times with EBM-2 to remove non-adherent erythrocytes. The number of adherent erythrocyte was counted on light microscope. The experiments were performed in triplicate and 28 fields were selected randomly to count erythrocyte number.

***Ex vivo* PS exposure measurement and venous thrombosis animal model**

Male Sprague-Dawley rats (SamTako Co., Osan, Korea) weighing 180-250 g were used for animal studies. For the measurement of PS exposure, 1 hr after intravenous injection of saline (vehicle) or $HgCl_2$ (bolus, 1.0 and 2.5 mg/kg/0.3 mL) into a left

femoral vein, blood was collected from the abdominal aorta using 3.8% trisodium citrate as anticoagulant. An aliquot of blood sample was diluted 200 fold with the buffer (10 mM HEPES-Na, 136 mM NaCl, 2.7 mM KCl, 2.0 mM $MgCl_2$, 1.0 mM NaH_2PO_4, 5.0 mM dextrose, 5 mg/ml BSA, 2.5 mM $CaCl_2$, pH 7.4) and was stained with annexin V-FITC for 15 min in the dark. PS exposure was measured as described above.

Venous thrombosis was induced by stasis combined with hypercoagulability. Rats (180-250 g) were anesthetized with urethane (1.25 g/kg, *i.p.*), the abdomen was surgically opened, and the vena cava was exposed after careful dissection. Two loose cotton threads were prepared 16 mm apart around the vena cava. All side branches were ligated tightly with cotton threads. One hr after intravenous injection of saline or $HgCl_2$ (bolus, 0.25, 0.5 and 1.0 mg/kg/0.3 mL) into a left femoral vein, 1,000-fold diluted thromboplastin was infused to induce thrombus formation. Stasis was initiated by tightening the two threads, first the proximal and after 30 sec, the distal one. The abdominal cavity was provisionally closed and blood stasis was maintained for 15 min. After the abdomen was reopened, the ligated venous segment was excised and opened longitudinally to remove the thrombus. Isolated thrombus was blotted of excess blood and immediately weighed.

Statistical analysis

The means and standard errors of means were calculated for all treatment groups. The data were subjected to one-way analysis of variance (ANOVA) followed by Duncan's multiple range test to determine which means were significantly different from the control. In all cases, a p value of < 0.05 was used to determine significance.

Results

To investigate the effects of mercury on erythrocytes, we examined the shape change in erythrocytes after exposure to 5 μM $HgCl_2$, using scanning electron microscopy (SEM). As seen in Figure 1A, normal discocytic shapes changed into echinocytic erythrocytes and further into spherocytes, depending on the exposure time to Hg^{2+}. It is well known that erythrocytes change into spherocytes by a substantial loss of membrane surface through vesiculation and microvesicle (MV) generation. In order to visually identify MV generation, erythrocytes attached to a poly-*l*-lysine coated coverslip chamber were treated with Hg^{2+} and observed under confocal microscopy using erythrocyte-specific anti-glycophorin-A-FITC. As a result, Hg^{2+} treatment induced typical MV generation on erythrocyte membranes (arrow, Figure 1B right). In the flow cytometry analysis, MV generation increased in a time and concentration dependent manner with Hg^{2+} incubation (Figure 1C and 1D).

MV bearing phosphatidylserine (PS) can display procoagulant activity. In the flow cytometry analysis with annexin V-FITC to specifically detect PS, MV generated by Hg^{2+} treatment were shown to express PS in their outer membranes (Figure 2A). Moreover, remnant erythrocytes also expressed PS in outer membrane (62.2 ± 11.2% at 5 μM Hg^{2+}, Figure 2B) consistent with the previous report by Eisele et al. (Eisele et al. 2006). PS expression also increased in a time dependent manner with Hg^{2+} (inset of Figure 2B), and of particular note, prolonged exposure induced significant PS expression even at lower concentrations of Hg^{2+} (down to 0.25 μM) (Figure 2C). To investigate the mechanism underlying Hg^{2+} induced PS exposure and MV generation, the activities of representative aminolipid translocases governing lipid asymmetry were evaluated. Flippase, an enzyme that recovers PS into the inner leaflet of the cell

membrane, and scramblase, an enzyme that disrupts lipid symmetry in the cell membrane, were measured based on the extent of NBD-PS and NBD-PC translocation, respectively after incubation of Hg^{2+}. NBD-PS and NBD-PC are the fluorescent analogs of PS and PC and the internalization of NBD-PS and NBD-PC by flippase and scramblase, respectively was measured by comparing the fluorescence intensity associated with the cells before and after BSA back-extraction as described in methods. As shown in Figure 2D and 2E, flippase was inhibited by Hg^{2+} while scramblase was activated in a concentration dependent manner which explains well Hg^{2+} -induced PS exposure.

Intracellular calcium increase can mediate concomitant inhibition of flippase and activation of scramblase, leading to the disruption of membrane lipid asymmetry (Daleke 2003). To investigate whether Hg^{2+} treatment can induce calcium increase, Fluo-4 loaded erythrocytes were incubated with Hg^{2+} and intracellular calcium increase was measured by flow cytometry analysis. As shown in Figure 3A, Hg^{2+} treatment increased intracellular calcium prominently up to 10 times the basal level. In this calcium signal, an artifactual increase due to possible interference with Fluo-4 binding by Hg^{2+} could be excluded by adding the Hg^{2+} quencher, TPEN, a high affinity membrane-permeable intracellular heavy metal chelator (Arslan et al. 1985). ATP depletion, which can prompt flippase inhibition, was also induced by Hg^{2+} (Figure 3B). In general, Hg^{2+} induced cytotoxicity is mediated by thiol depletion (Zalups 2000) or oxidative stress (Wiggers et al. 2008). To examine the role of thiol depletion and oxidative stress in Hg^{2+}-induced PS-exposure and MV generation, erythrocytes were pre-incubated with thiol-supplements, N-acetylcysteine and DTT or the antioxidant, Trolox. As shown in Figure 3C, while Trolox was marginally effective,

thiol-supplements effectively blocked Hg^{2+}-induced PS exposure and MV generation, indicating a major role of thiol depletion. Indeed, Hg^{2+} treatment induced significant thiol depletion (Figure 3E). In line with these findings, thiol-supplementation prevented Hg^{2+}-induced ATP depletion and Ca^{2+} increase (Figure 3F) indicating that Hg^{2+} induces PS exposure and MV generation in erythrocytes through protein thiol depletion-mediated ATP depletion and Ca^{2+} increases.

Prothrombotic effects of Hg^{2+}-induced PS exposure and MV generation was confirmed by evidence of increased thrombin generation based on the prothrombinase assay and thrombin generation in plasma (Figure 4A and 4B). Moreover, increased adherence of Hg^{2+}-exposed erythrocytes to endothelial cells was demonstrated by increased erythrocyte adhesion on human umbilical vein endothelial cells (HUVEC, Figure 4C). To evaluate the *in vivo* relevance of Hg^{2+}-induced procoagulant activity in erythrocytes, rat *ex vivo* PS exposure measurement and *in vivo* venous thrombosis models were used. Before the *in vivo* experiments, PS exposure and MV generation by Hg^{2+} were confirmed in rat erythrocytes (Figure 5A) which showed a similar pattern to human erythrocytes. Confirming these *in vitro* results, treatment of $HgCl_2$ (i.v. bolus 0.25 – 2.5 mg/kg (0.92 – 9.2 μmoles/kg)) induced PS exposure on erythrocytes *ex vivo* (Figure 5B, 2.1 ± 0.2% in 1 mg/kg and 3.4 ± 0.7% in 2.5 mg/kg $HgCl_2$ *vs* 1.4 ± 0.1% in vehicle, $p < 0.05$) and promoted clot formation in a stasis- and hypercoagulability-induced venous thrombosis model following thromboplastin infusion (Figure 5C, 12.2 ± 1.0 mg in 0.5 mg/kg and 16.9 ± 2.3 mg in 1 mg/kg $HgCl_2$ *vs* 2.4 ± 1.7 mg in vehicle, $p < 0.01$), suggesting that Hg^{2+}-induced procoagulant activity in erythrocytes could contribute to increased thrombosis *in vivo*.

Discussion

In this study, we demonstrated that Hg^{2+} can induce shape changes, MV generation and PS exposure on erythrocytes, important mediators of procoagulant activation of erythrocytes. Hg^{2+}- mediated thiol-depletion was responsible for calcium increase- and ATP depletion-mediated flippase inhibition and scramblase activation, leading to increased thrombin generation, enhanced adhesion of erythrocytes to endothelial cells and ultimately, accelerated thrombus formation (Figure 6). Most importantly, *ex vivo* PS exposure measurement and the rate *in vivo* venous thrombosis model confirmed the procoagulant effect of Hg^{2+} by demonstrating increased PS exposure and clot formation, suggesting that procoagulant activation of erythrocytes might contribute to cardiovascular diseases (CVDs) associated with mercury exposure.

Erythrocytes can contribute to haemostasis and thrombosis through procoagulant activation via PS exposure and MV generation (Zwaal and Schroit 1997; Zwaal et al. 2005). Endogenous thrombogenic substances such as arachidonic acid, lysophosphatic acid, and thromboxane are known to induce PS exposure on erythrocyte surfaces (Chung et al. 2007; Valles et al. 2002). In addition, we demonstrated previously that another toxic heavy metal, lead (Pb), can induce a substantial level of PS exposure in erythrocytes, and that this procoagulant activity was manifested as enhanced thrombus formation (Shin et al. 2007). Interestingly, it is well-known that erythrocytes can be a preferential store for toxic heavy metals. Methylmercury accumulates into erythrocytes at a concentration more than 20 times that of plasma (Clarkson 2002) and 90% of body lead is associated with erythrocytes. These findings suggest that erythrocytes can be a common target for CV toxicity of heavy metals and that the content of heavy metals in or the role of erythrocytes should be more closely investigated in relation to CV toxicity

of heavy metals.

Previously, it has been reported that millimolar concentrations of Hg^{2+} induces shape changes and hemolysis in erythrocytes (Suwalsky et al. 2000; Zolla et al. 1997). The concentration employed in these studies, however, was unrealistically high, considering reported human exposure levels even in the highly contaminated areas. In the current study, however, we discovered that longer exposure to concentrations of Hg^{2+} as low as 0.25 μM can induce shape changes and procoagulant activation in erythrocytes as determined by increased PS exposure. The highest blood mercury concentrations reported in humans were in workers in the gold-mines of the Amazon area (Akagi et al. 1995) whose blood mercury levels were as high as 150 μg/L (~0.75 μM). Wierzbicki et al. (2002) reported that workers occupationally exposed to mercuric vapors exhibited a statistically significant increase in blood coagulation along with increased thrombin generation. Their average plasma mercury levels were around 0.03 to 0.04 μM but measured as high as 83.3 μg/L (0.4 μM). According to the report of Virtanen et al. (2005), increased CV events were observed in a mercury-exposed population with an average hair mercury level of 1.9 μg/g (0 to 15.7 μg/g), which is estimated to indicate a blood mercury level of 9.5 μg/L (0.05 μM) based on a 200:1 hair to blood mercury ratio (Budtz-Jorgensen et al. 2004). These levels are within an order or magnitude of the mercury concentrations used in our study, suggesting that mercury-induced procoagulant activation of erythrocytes might indeed contribute to the increased CVDs in human populations. However, as this study was conducted only with Hg^{2+}, further *in vivo* studies with methylmercury or elemental mercury are needed to fully clarify the link between mercury-mediated procoagulant activation of erythrocytes

and mercury-associated CVDs.

Further to the previous report on Hg^{2+}-induced echinocyte in human erythrocytes (Suwalsky et al. 2000), we newly discovered that echinocytes can be further progressed into spherocytes (Figure 1A) by prolonged exposure to Hg^{2+}. Moreover, along with these remarkable shape changes, substantial amounts of MV can be liberated from erythrocytes. Apart from clot-promoting activity in plasma, MV generation can result in decreased deformability of erythrocytes (Chabanel et al. 1989; Chasis and Mohandas 1986; Mentzer et al. 1987) and more importantly, PS-exposing MV provide sites for adhesion of platelets and neutrophils by localizing at subendothelium, indicating that Hg^{2+}-induced MV generation can contribute to the prothrombotic effects of mercury exposure.

In our study, thiol-depletion was determined to be a key mediator for the calcium increase, ATP depletion, PS exposure and MV generation in erythrocytes by Hg^{2+}. Thiol-depletion by Hg^{2+} can be well explained by the strong thiol-binding affinity of nucleophilic Hg^{2+} (Casarett 2007). Intracellular molecules with free sulfhydryl groups, such as glutathione, cysteine and metallothionein can be an easy target for Hg^{2+} binding and free thiol groups of intracellular proteins, vital to the maintenance of erythrocyte integrity (e.g., of the cytoskeleton) and ionic balance (e.g., Na^{2+}-K^{+} ATPase) can be readily modified by thiol-depleting agents, leading to a increased fragility of the erythrocyte membrane and the disruption of ionic homeostasis. Moreover, it is well-known that depletion of free thiols in cells can cause depletion of ATP, inhibition of flippase (Daleke and Lyles 2000) and increased calcium, consistent with the result of current study.

In conclusion, we demonstrated that low dose mercury can induce thrombogenic

PS exposure and MV generation through thiol-depletion-mediated ATP depletion and calcium increase in erythrocytes. As shown by increased PS exposure and clot formation *in vivo*, we believe that mercury-induced procoagulant activation of erythrocytes might contribute to enhanced thrombosis in the population exposed to mercury, providing an important clue for the elucidation for the CVDs associated with mercury.

References

ASTDR. 2007. Toxicological profile for mercury. Agency for Toxic Substances and Disease Registry, US Public Health Service, Atlanta, GA.

Akagi H, Malm O, Branches FJP, Kinjo Y, Kashima Y, Guimaraes JRD, et al. 1995. Human exposure to mercury due to goldmining in the Tapajos River basin, Amazon, Brazil: Speciation of mercury in human hair, blood and urine. Water, Air, & Soil Pollution 80: 85-94.

Arslan P, Di Virgilio F, Beltrame M, Tsien RY, Pozzan T. 1985. Cytosolic Ca^{2+} homeostasis in Ehrlich and Yoshida carcinomas. A new, membrane-permeant chelator of heavy metals reveals that these ascites tumor cell lines have normal cytosolic free Ca^{2+}. J Biol Chem 260: 2719-2727.

Berglund M, Lind B, Bjornberg K, Palm B, Einarsson O, Vahter M. 2005. Inter-individual variations of human mercury exposure biomarkers: a cross-sectional assessment. Environ Health: A Global Access Science Source 4: 20.

Berlin M, Zalups RK, Fowler BA, Gunnar FN, Bruce AF, Monica N, et al. 2007. Mercury. In: Handbook on the Toxicology of Metals. 3rd ed. Burlington: Academic Press, 675-729.

Budtz-Jorgensen E, Grandjean P, Jorgensen PJ, Weihe P, Keiding N. 2004. Association between mercury concentrations in blood and hair in methylmercury-exposed subjects at different ages. Environ Res 95: 385-393.

Casarett LJ, Klaassen, Curtis. D., John Doull. 2007. Casarett and Doull's Toxicology: the basic science of poisons. 7th ed. New York: Mcgraw-Hill

Chabanel A, Sung KL, Rapiejko J, Prchal JT, Palek J, Liu SC, et al. 1989. Viscoelastic properties of red cell membrane in hereditary elliptocytosis. Blood 73: 592-595.

Chasis JA, Mohandas N. 1986. Erythrocyte membrane deformability and stability: two distinct membrane properties that are independently regulated by skeletal protein associations. J Cell Biol 103: 343-350.

Chung SM, Bae ON, Lim KM, Noh JY, Lee MY, Jung YS, et al. 2007. Lysophosphatidic acid induces thrombogenic activity through phosphatidylserine exposure and procoagulant microvesicle generation in human erythrocytes. Arterioscler Thromb Vasc Biol 27: 414-421.

Clarkson TW. 2002. The three modern faces of mercury. Environ Health Perspect 110 Suppl 1: 11-23.

Clarkson TW, Magos L, Myers GJ. 2003. The toxicology of mercury--current exposures and clinical manifestations. N Engl J Med 349: 1731-1737.

Closse C, Dachary-Prigent J, Boisseau MR. 1999. Phosphatidylserine-related adhesion of human erythrocytes to vascular endothelium. Br J Haematol 107: 300-302.

Daleke DL, Lyles JV. 2000. Identification and purification of aminophospholipid flippases. Biochim Biophys Acta 1486: 108-127.

Daleke DL. 2003. Regulation of transbilayer plasma membrane phospholipid asymmetry. J Lipid Res 44: 233-242.

Di Monte D, Bellomo G, Thor H, Nicotera P, Orrenius S. 1984. Menadione-induced cytotoxicity is associated with protein thiol oxidation and alteration in intracellular Ca^{2+} homeostasis. Arch Biochem Biophys 235: 343-350.

Eisele K, Lang PA, Kempe DS, Klarl BA, Niemoller O, Wieder T, et al. 2006. Stimulation of erythrocyte phosphatidylserine exposure by mercury ions. Toxicol Appl Pharmacol 210: 116-122.

Environment Canada. 2004. Mercury and the environment: sources of mercury. http://www.ec.gc.ca/MERCURY/EN/bf.cfm.

Hilarius PM, Ebbing IG, Dekkers DW, Lagerberg JW, de Korte D, Verhoeven AJ. 2004. Generation of singlet oxygen induces phospholipid scrambling in human erythrocytes. Biochemistry 43: 4012-4019.

Houston MC. 2007. The role of mercury and cadmium heavy metals in vascular disease, hypertension, coronary heart disease, and myocardial infarction. Altern Ther Health Med 13: S128-133.

Macfarlane DE. 1981. The effects of methyl mercury on platelets: induction of aggregation and release via activation of the prostaglandin synthesis pathway. Mol Pharmacol 19: 470-476.

Mahaffey KR, Mergler D. 1998. Blood levels of total and organic mercury in residents of the upper St. Lawrence River basin, Quebec: association with age, gender, and fish consumption. Environ Res 77: 104-114.

Martinez MC, Tesse A, Zobairi F, Andriantsitohaina R. 2005. Shed membrane microparticles from circulating and vascular cells in regulating vascular function. Am J Physiol Heart Circ Physiol 288: H1004-1009.

McKelvey W, Gwynn RC, Jeffery N, Kass D, Thorpe LE, Garg RK, et al. 2007. A

biomonitoring study of lead, cadmium, and mercury in the blood of New York city adults. Environ Health Perspect 115: 1435-1441.

Mentzer WC, Jr., Iarocci TA, Mohandas N, Lane PA, Smith B, Lazerson J, et al. 1987. Modulation of erythrocyte membrane mechanical stability by 2,3-diphosphoglycerate in the neonatal poikilocytosis/elliptocytosis syndrome. J Clin Invest 79: 943-949.

Peyrou V, Lormeau JC, Herault JP, Gaich C, Pfliegger AM, Herbert JM. 1999. Contribution of erythrocytes to thrombin generation in whole blood. Thromb Haemost 81: 400-406.

Rodrigues JL, de Souza SS, de Oliveira Souza VC, Barbosa Jr F. 2010. Methylmercury and inorganic mercury determination in blood by using liquid chromatography with inductively coupled plasma mass spectrometry and a fast sample preparation procedure. Talanta 80: 1158-1163.

Salonen JT, Seppanen K, Lakka TA, Salonen R, Kaplan GA. 2000. Mercury accumulation and accelerated progression of carotid atherosclerosis: a population-based prospective 4-year follow-up study in men in eastern Finland. Atherosclerosis 148: 265-273.

Shin JH, Lim KM, Noh JY, Bae ON, Chung SM, Lee MY, et al. 2007. Lead-induced procoagulant activation of erythrocytes through phosphatidylserine exposure may lead to thrombotic diseases. Chem Res Toxicol 20: 38-43.

Suwalsky M, Ungerer B, Villena F, Cuevas F, Sotomayor CP. 2000. $HgCl_2$ disrupts the structure of the human erythrocyte membrane and model phospholipid bilayers. J Inorg Biochem 81: 267-273.

Trasande L, Landrigan PJ, Schechter C. 2005. Public health and economic consequences of methyl mercury toxicity to the developing brain. Environ Health Perspect 113: 590-596.

Valera B, Dewailly E, Poirier P. 2008. Cardiac autonomic activity and blood pressure among Nunavik Inuit adults exposed to environmental mercury: a cross-sectional study. Environmental Health 7: 29.

Valles J, Santos MT, Aznar J, Martinez M, Moscardo A, Pinon M, et al. 2002. Platelet-erythrocyte interactions enhance alpha(IIb)beta(3) integrin receptor activation and P-selectin expression during platelet recruitment: down-regulation by aspirin ex vivo. Blood 99: 3978-3984.

Virtanen JK, Voutilainen S, Rissanen TH, Mursu J, Tuomainen TP, Korhonen MJ, et al. 2005. Mercury, fish oils, and risk of acute coronary events and cardiovascular disease,

coronary heart disease, and all-cause mortality in men in eastern Finland. Arterioscler Thromb Vasc Biol 25: 228-233.

Virtanen JK, Rissanen TH, Voutilainen S, Tuomainen TP. 2007. Mercury as a risk factor for cardiovascular diseases. J Nutr Biochem 18: 75-85.

Wierzbicki R, Prazanowski M, Michalska M, Krajewska U, Mielicki WP. 2002. Disorders in blood coagulation in humans occupationally exposed to mercuric vapors. J Trace Elem Exp Med 15: 21-29.

Wiggers GA, Pecanha FM, Briones AM, Perez-Giron JV, Miguel M, Vassallo DV, et al. 2008. Low mercury concentrations cause oxidative stress and endothelial dysfunction in conductance and resistance arteries. Am J Physiol Heart Circ Physiol 295: H1033-H1043.

Zalups RK. 2000. Molecular interactions with mercury in the kidney. Pharmacol Rev 52: 113-143.

Zolla L, Lupidi G, Bellelli A, Amiconi G. 1997. Effect of mercuric ions on human erythrocytes. Relationships between hypotonic swelling and cell aggregation. Biochim Biophys Acta 1328: 273-280.

Zwaal RF, Comfurius P, van Deenen LL. 1977. Membrane asymmetry and blood coagulation. Nature 268: 358-360.

Zwaal RF, Schroit AJ. 1997. Pathophysiologic implications of membrane phospholipid asymmetry in blood cells. Blood 89: 1121-1132.

Zwaal RF, Comfurius P, Bevers EM. 2005. Surface exposure of phosphatidylserine in pathological cells. Cell Mol Life Sci 62: 971-988.

Legends

Figure 1. Mercury-induced shape changes in human erythrocytes.

(A) Erythrocytes were incubated with 5 μM Hg^{2+} up to 4 hr at 37°C. The cells were fixed and the morphological changes were examined under SEM. Representative microscopic photographs of 3 independent experiments from different blood donors are shown here. (scale bar: 5 μm) (B) Erythrocytes, attached to poly-*l*-lysine coated coverslip chamber, were treated with Hg^{2+} (5 μM) for 1 hr and observed under confocal microscopy using erythrocyte-specific anti-glycophorin-A-FITC. (C) After erythrocytes were incubated with Hg^{2+} for 4 hr at 37°C, erythrocytes and MV were identified by forward scatter characteristics (FSC) in a representative dot plot (Hg^{2+} 5 μM). (D) Time and (E) concentration-dependent increases in MV generation with Hg^{2+} incubation. Values are mean ± SEM of three to five independent experiments. * significantly different from the control ($p < 0.05$).

Figure 2. PS exposure in MV and remnant erythrocytes by Hg^{2+} and the effects of Hg^{2+} treatment on the aminophospholipid translocation.

After human erythrocytes were incubated with distilled water (DW) (control) or Hg^{2+} at 37°C , flow cytometric analysis was performed. (A) Representative histogram of remnant cells and MV expressing PS. (B) and (C) Time and concentration-dependent PS exposure on erythrocytes by Hg^{2+}. After erythrocytes were incubated with DW (Control) or 1, 2 and 5 μM Hg^{2+} for 1 hr at 37°C the extent of phospholipid translocation was measured. (D) C6-NBD PS translocation by flippase and (E) C6-NBD PC translocation by scramblase. Values are mean ± SEM of three independent

experiments. * significantly different from the control ($p < 0.05$).

Figure 3. Effects of Hg^{2+} on intracellular Ca^{2+}, ATP and protein thiol in human erythrocytes.

(A) Erythrocytes loaded with Fluo-4 were incubated with DW (control) or 1, 2 and 5 μM Hg^{2+}. After 4 hr incubation at 37°C, intracellular Ca^{2+} levels were evaluated by flow cytometry. To exclude the interference from intracellular Hg^{2+}, samples were evaluated in the presence of 100 μM TPEN. (B) After erythrocytes were incubated with DW (control) or 1, 2 and 5 μM Hg^{2+} for 4 hr at 37°C, levels of intracellular ATP were measured by a bioluminescent assay. (C and D) Human erythrocytes were pretreated with 0.5 mM NAC or 0.5 mM DTT (thiol supplements) or 100 μM Trolox (antioxidant) 5 min prior to Hg^{2+} treatment. After incubation of the pretreated erythrocytes with 5 μM Hg^{2+}, (C) PS exposure and (D) MV generation were measured by flow cytometry analysis. (E) Protein thiol was measured using DTNB method. (F) Inhibition of Ca^{2+} increase (left) and ATP depletion by thiol-supplements (right). Values are the mean ± SEM of three independent experiments. * significantly different from the control ($p < 0.05$).

Figure 4. Enhancement of thrombin generation and erythrocyte adherence to endothelial cell by Hg^{2+} treatment.

(A) After erythrocytes were incubated with DW (control) or 1, 2 and 5 μM Hg^{2+} for 4 hr at 37°C, aliquots were subjected to the prothrombinase assay. (B) Hg^{2+}-treated erythrocytes were added to human plasma and thrombin generation was initiated by recombiplastin. (C) Hg^{2+}-treated erythrocytes were incubated with HUVECs for 45 min.

After washing, adhered erythrocytes to HUVECs were counted on microscope. Values are the mean ± SEM of three to five independent experiments. * significantly different from the control ($p < 0.05$).

Figure 5. Effects of Hg^{2+} on PS exposure and thrombus formation in *in vivo* rat animal model.

After rat erythrocytes were treated with DW (control) or 1, 2, 5 μM Hg^{2+} for 4 hr at 37°C, (A) the extent of MV generation and PS exposure were measured by flow cytometry. After i.v. administration of saline (control) or mercuric chloride (0.25 - 2.5 mg/kg), (B) the extent of PS exposure on erythrocytes was measured in whole blood using flow cytometry, and (C) thrombus formation was induced by the infusion of thromboplastin in a rat venous thrombosis model. Values are the mean ± SEM of four independent experiments. * significantly different from the control ($p < 0.05$).

Figure 6. Suggested mechanism of Hg^{2+}-induced procoagulant activation of erythrocytes.

Hg^{2+} induces procoagulant activation of erythrocytes and enhanced thrombus formation through thrombogenic phosphatidylserine (PS) exposure and microvesicle (MV) generation mediated by protein-thiol depletion, ATP depletion and Ca^{2+} increase via scramblase activation and flippase inhibition.

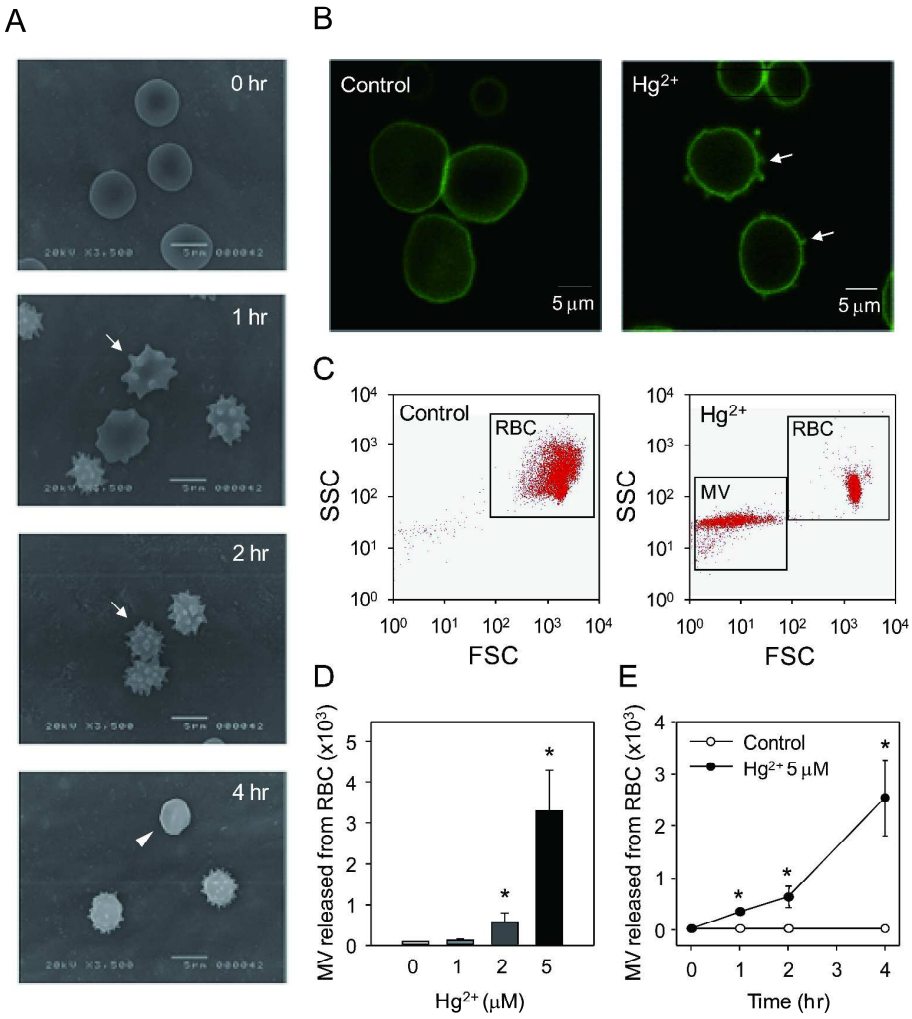

Figure 1

215x246mm (600 x 600 DPI)

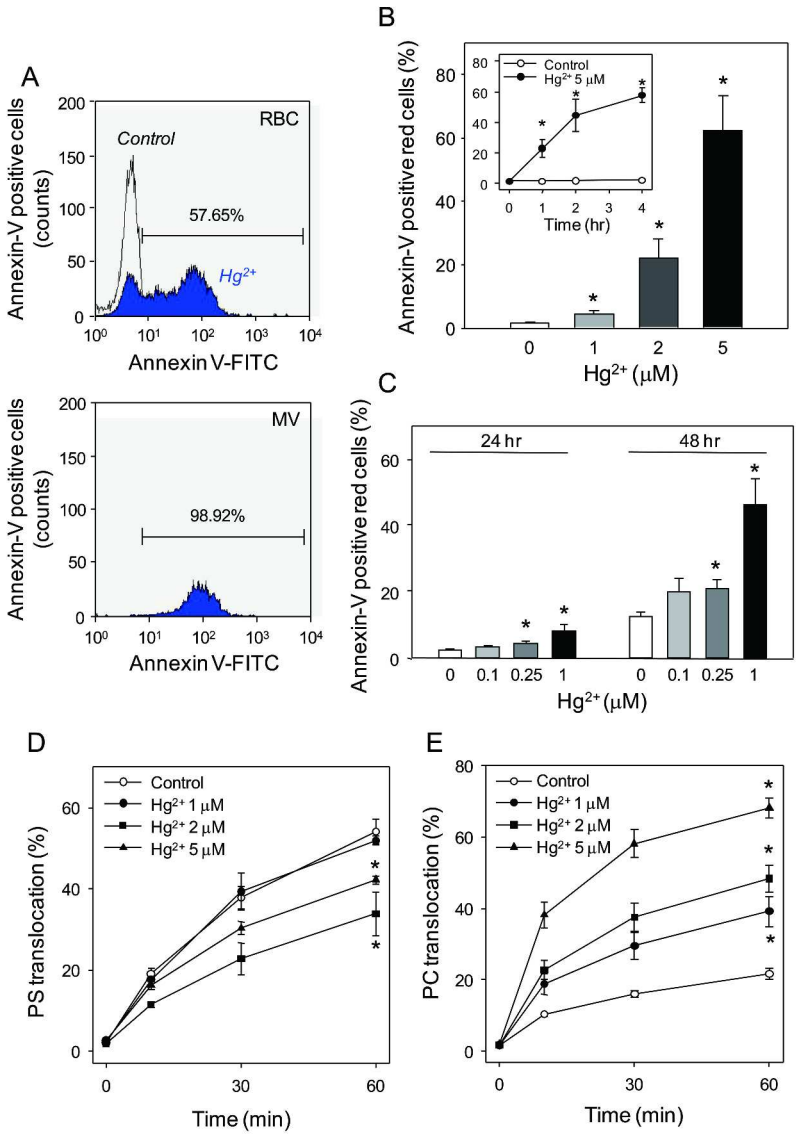

Figure 2

215x317mm (300 x 300 DPI)

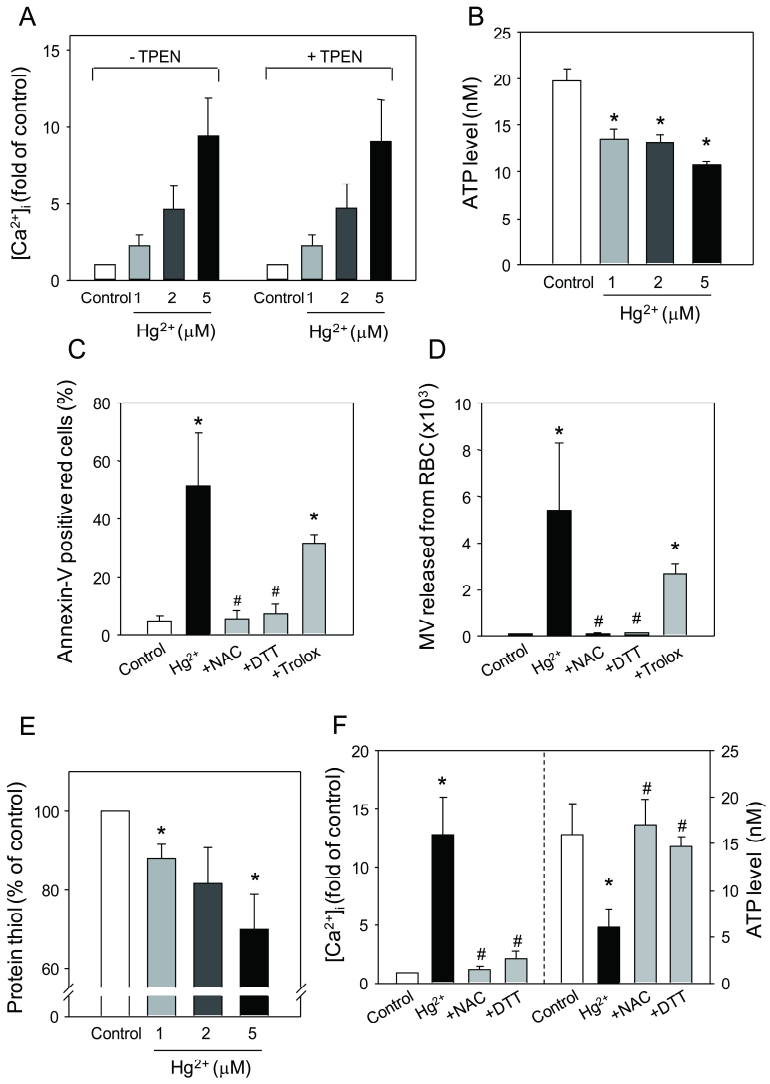

Figure 3

215x279mm (600 x 600 DPI)

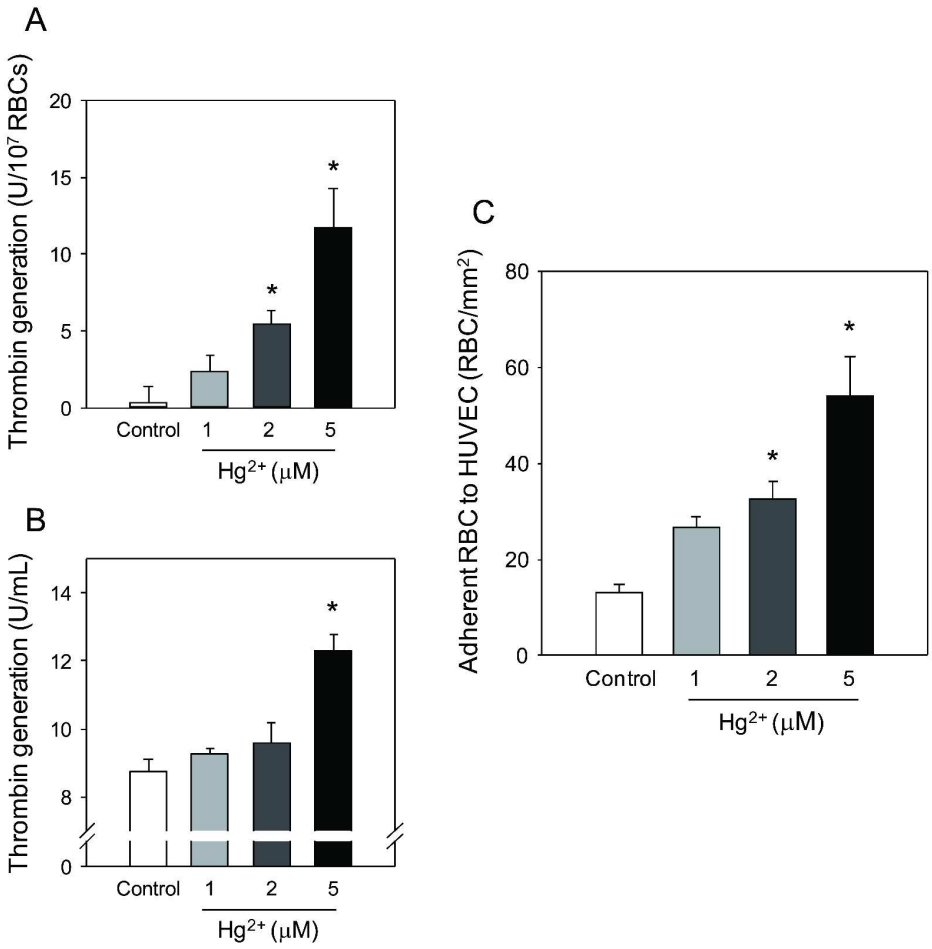

Figure 4

215x231mm (600 x 600 DPI)

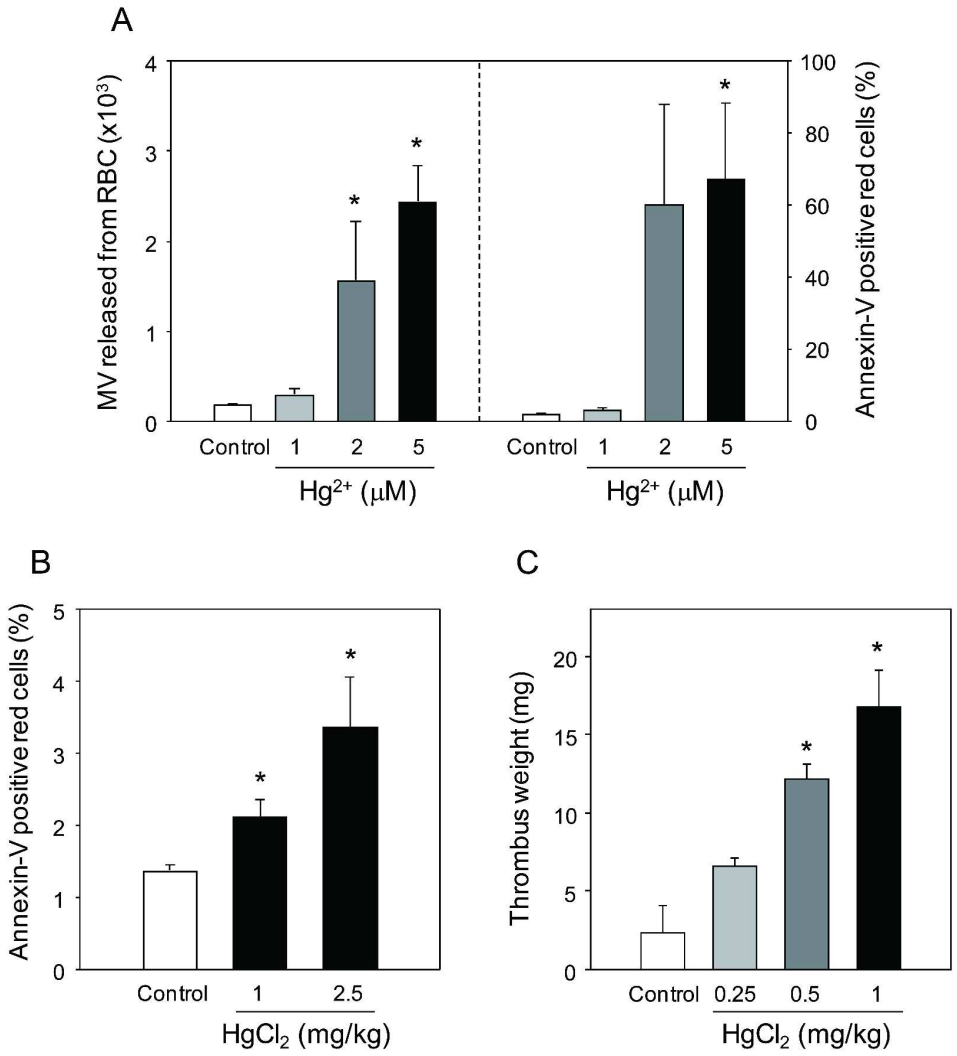

Figure 5

215x254mm (600 x 600 DPI)

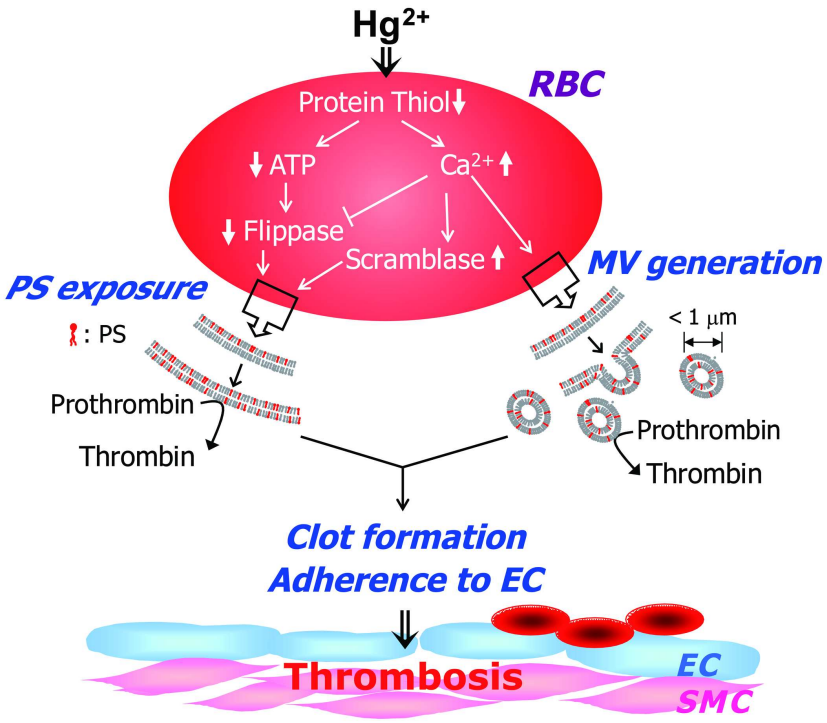

Figure 6

215x187mm (300 x 300 DPI)